

SOD1 is a Possible Predictor of COVID-19 Progression as Revealed by Plasma Proteomics

Benhong Xu, Yuxuan Lei, Xiaohu Ren, Feng Yin, Weihua Wu, Ying Sun, Xiaohui Wang, Qian Sun, Xifei Yang, Xin Wang, Renli Zhang, Zigang Li,* Shisong Fang,* and Jianjun Liu*



Cite This: *ACS Omega* 2021, 6, 16826–16836



Read Online

ACCESS |



Metrics & More

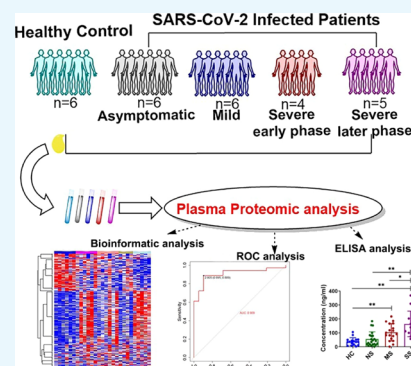


Article Recommendations



Supporting Information

ABSTRACT: The coronavirus disease 2019 (COVID-19) pandemic caused by severe acute respiratory syndrome coronavirus 2 (SARS-CoV-2) has become a worldwide health emergency. Patients infected with SARS-CoV-2 present with diverse symptoms related to the severity of the disease. Determining the proteomic changes associated with these diverse symptoms and in different stages of infection is beneficial for clinical diagnosis and management. Here, we performed a tandem mass tag-labeling proteomic study on the plasma of healthy controls and COVID-19 patients, including those with asymptomatic infection (NS), mild syndrome, and severe syndrome in the early phase and the later phase. Although the number of patients included in each group is low, our comparative proteomic analysis revealed that complement and coagulation cascades, cholesterol metabolism, and glycolysis-related proteins were affected after infection with SARS-CoV-2. Compared to healthy controls, ELISA analysis confirmed that SOD1, PRDX2, and LDHA levels were increased in the patients with severe symptoms. Both gene set enrichment analysis and receiver operator characteristic analysis indicated that SOD1 could be a pivotal indicator for the severity of COVID-19. Our results indicated that plasma proteome changes differed based on the symptoms and disease stages and SOD1 could be a predictor protein for indicating COVID-19 progression. These results may also provide a new understanding for COVID-19 diagnosis and treatment.



INTRODUCTION

Coronavirus disease 2019 (COVID-19), caused by the newly identified severe acute respiratory distress syndrome-associated coronavirus-2 (SARS-CoV-2), is threatening the whole human population worldwide. The virus was declared a global pandemic by the World Health Organization (WHO) in March 2020.¹ As of March 16, 2021, more than 120 million people have been infected by the virus and more than 2 million people have lost their lives, according to CDC reports.² A comprehensive understanding of the molecular characteristics of patients with different symptoms after infection with SARS-CoV-2 is vital for effective management of the disease.

Patients with confirmed SARS-CoV-2 infection develop diverse symptoms, including fever, cough, and fatigue.^{3,4} Although chest radiography and reverse transcriptase-polymerase chain reaction are effective and widely used methods for the confirmation of SARS-CoV-2 infection, these techniques cannot be used to reveal the molecular mechanism or predict disease progression. Proteomics has been widely used to identify biomarkers and disease progression for various diseases, including infectious diseases.^{5–7} The serum biomarkers from patients with severe acute respiratory syndrome (SARS) were also identified by proteomics.^{8,9} Thus, proteomics is a promising approach to identify biomarkers of COVID-19.

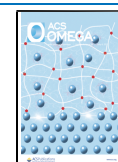
It has been widely accepted that plasma could be used to reflect pathophysiological alterations in disease progression. The illness of COVID-19 is classified as asymptomatic, mild symptoms, or severe symptoms based on the clinical status.¹⁰ Age and coexisting illness have been reported to increase the severity of pneumonia.^{11,12} A combination of biomarkers for the prediction of different clinical outcomes of COVID-19 patients has been revealed by the proteomic study.¹³ Another elegant proteomic study also reported that the dysregulation of macrophages, platelet degranulation, and complement system pathways were detected in the sera of COVID-19 patients.¹⁴ Recently, a number of proteomic and metabolic studies extended our knowledge of the plasma proteome and metabolite changes in COVID-19 patients.^{9,15,16} However, our knowledge on the prediction and treatment of COVID-19 is still limited.

In this study, we fully investigated the proteome changes in COVID-19 patients with asymptomatic infection, mild

Received: March 15, 2021

Accepted: June 10, 2021

Published: June 24, 2021



syndrome (MS), and severe syndrome in the early phase and later phase. We identified changes in hundreds of plasma proteins in these patients and for the first time we provided evidence that SOD1 can be used to predict COVID-19 progression. These results increase our understanding of SARS-CoV-2 infection and its diagnosis.

MATERIALS AND METHODS

Reagents. The following reagents were used in this study: proteinase inhibitor cocktail (Roche, BS, CH), tandem mass tag (TMT)-labeling kits (Thermo Scientific, NJ, USA), sequencing-grade trypsin/LyC mixture (Promega, WI, USA), and enzyme-linked immunosorbent assay (ELISA) kits for SOD1, LDHA, and PRDX2 (Cloud-Clone Corporation, Wuhan, China).

Plasma Sample Collection. Disease severity classification was defined according to the China National Health Commission Guidelines for Diagnosis and Treatment of 2019-nCoV infection.¹⁷ Patients with symptomatic infection (NS, $n = 6$), MS ($n = 6$), severe syndrome in the early phase (SSEP, $n = 4$), severe syndrome in the later phase (SSLP, $n = 5$), and healthy controls (HCs, $n = 6$) were enrolled in the proteomic study (Table 1). Detailed information for the

Table 1. COVID-19 Patient Information for Proteomic Study

experiment	groups	mean age (SD)	sex M/F
TMT	healthy control ($n = 6$)	29.50 (16.92)	2/4
	asymptomatic ($n = 6$)	19.33 (14.46)	4/2
	mild symptom ($n = 6$)	39.83 (13.64)	3/3
	severe symptom in early phase ($n = 4$)	54.25 (12.42)	1/3
	severe symptom in later phase ($n = 5$)	57.60 (13.11)	2/3
ELISA	healthy control ($n = 19$)	37.63 (8.88)	13/6
	asymptomatic ($n = 24$)	23.25 (12.10)	9/15
	mild symptom ($n = 20$)	43.35 (16.89)	10/10
	severe symptom ($n = 15$)	59.07 (12.54)	6/9

patients used in the proteomic and ELISA analysis is listed in Supporting Information Table S6. All plasma samples from COVID-19 patients and HCs were collected from the Shenzhen Center for Disease Control and Prevention. All the experiments were performed in BSL-3 facilities before the virus was inactivated in accordance with management practices. This research was approved by the ethics committee of the Shenzhen Center for Disease Control and Prevention [approval number: 2020-025A; 2021-001A].

High-Abundance Protein Removal. High-abundance proteins were isolated using a PureProteome Human Albumin/Immunoglobulin Depletion kit (Millipore) according to the manufacturer's instructions. Plasma protein concentration was detected using a NanoDrop 2000C (Thermo Scientific, NJ, USA).

TMT Labeling. TMT labeling was performed according to a previously published method, with slight modifications.¹⁸ As shown in Figure 1A, each individual plasma sample is processed for the TMT-labeling study. Samples of proteins from each group (50 μ g) were reduced with 10 mM dithiothreitol for 1 h at 37 °C, followed by the addition of 25 mM 2-iodoacetamide for 30 min in the dark at room temperature. Samples were then digested with trypsin (1:100

w/w) and desalted by reversed-phase column chromatography (Oasis HLB; Waters, MC, USA) according to the manufacturer's instructions. After drying using a vacuum concentrator, each protein digest sample was redissolved in 100 μ L of triethylammonium bicarbonate buffer (200 mM, pH 8.5). Peptides were labeled using TMT reagents as follows: HC, TMT-126; NS, TMT-127; MS, TMT-128; SSEP, TMT-129; and SSLP, TMT-130. The reaction was kept at room temperature for 1 h and quenched by the addition of 5% hydroxylamine for 15 min. All the labeled peptides in each set were combined and then desalted, dried, and dissolved in 100 μ L of 0.1% formic acid (FA). Six sets of samples were subsequently separated into fractions using high-performance liquid chromatography (HPLC), respectively (Figure 1A).

HPLC Separation. TMT-labeled peptides were fractionated by HPLC (UltiMate 3000 UHPLC, Thermo Scientific). The gradient elution buffer consisted of 100% Milli-Q H₂O (phase A, pH 10.0) and 98% acetonitrile (phase B, pH 10.0). An XBridge BEH300 C18 column (4.6 \times 250 mm, 2.5 μ m, Waters) was used for peptide separation at a flow rate of 1 mL/min. The column was maintained at 45 °C, and peptide detection was performed by UV absorbance at 214 nm. Fractions were collected every 1.5 min in 45 tubes, dried, and combined into 15 tubes before being dissolved in 20 μ L of 0.1% FA for further liquid chromatography (LC)-tandem mass spectrometry (MS/MS) analysis.

Peptide Analysis by LC-MS/MS. The peptide fractions were analyzed by LC-MS/MS using a Q Exactive mass spectrometer (Thermo Scientific, NJ, USA) with a silica capillary column [75 μ m internal diameter (ID), 150 mm length; Upchurch, WA, USA] packed with C18 resin (300 Å, 5 μ L; Varian, Lexington, MA, USA). The Q Exactive mass spectrometer was operated with Xcalibur 2.1.2 software in the data-dependent acquisition mode. A single full-scan mass spectrum in Orbitrap (400–1, 800 m/z , 70,000 resolution) was followed by the top 20 data-dependent MS/MS scans at 27% normalized collision energy (higher-energy C-trap dissociation).

MS/MS spectra were searched against the UniProt_Homo sapiens database (download from the UniProt database on May 13th, 2020) using the SEQUEST search algorithms embedded into Proteome Discoverer 2.1 (Thermo Scientific). The search criteria were set according to the recommended parameters with the following alterations: trypsin was selected for protein digestion, two missed cleavage sites were allowed, static modifications were set as carbamidomethylation (C, +57.021 Da) and TMT6-plex (lysine [K] and any N-terminus of peptides), and oxidation (methionine, M) was set as dynamic modification. Additionally, 20 ppm was set as the precursor ion mass tolerance for all the mass spectrometry data acquired using the Orbitrap mass analyzer, and 20 mmu was used for the MS² spectral data. Proteins were used for a subsequent analysis when at least one unique peptide was identified, the false discover rate (FDR) was less than 1% and three replicates were quantified. Protein changes were evaluated by comparison of reporter ions from each group and the ratios were transformed into log₂(ratio), with 0.5 and -0.5 set as increased and decreased thresholds, respectively. The mass spectrometry proteomics data have been deposited in the ProteomeXchange Consortium via the PRIDE¹⁹ partner repository with the dataset identifier PXD024728 and 10.6019/PXD024728.

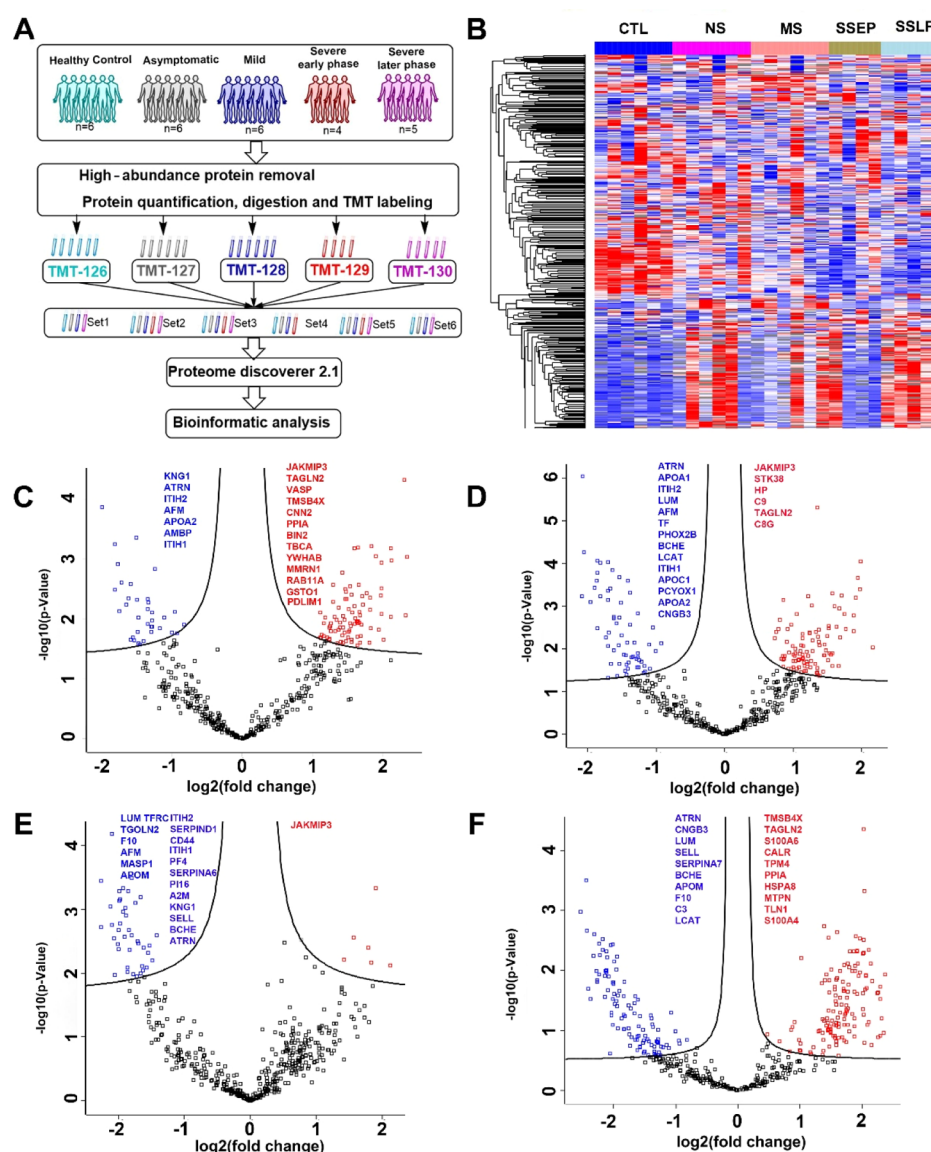


Figure 1. Proteomic landscape of plasma from COVID-19 patients. (A) TMT-labeling proteomic study on plasma of COVID-19 patients; plasma samples were divided into HC, asymptomatic (NS), MS, SSEP and SSLP groups. (B) Heatmap analysis of the identified and quantified proteins. High-abundance proteins are shown in red and low-abundance proteins are shown in blue. (C) Volcano plot analysis of the dysregulated proteins of NS patients. (D) Volcano plot analysis of dysregulated proteins of MS patients. (E) Volcano plot analysis of dysregulated proteins of SSEP patients. (F) Volcano plot analysis of dysregulated proteins of SSLP patients. The downregulated proteins are shown in blue and the upregulated proteins are shown in red.

Bioinformatics Analysis. All the scaled protein abundances were submitted to Peruses software for analysis. Z-score was used for protein abundance normalization and the subsequent heatmap and volcano plot analysis. The WEB-based GENE SeT Analysis Toolkit was used for Kyoto Encyclopedia of Genes and Genomes (KEGG) pathway analysis. All the changed proteins were analyzed using gene ontology (GO) web-based searching. STRING database version 10.0 (<http://string-db.org>) was used for protein–protein interaction (PPI) analysis with a confidence threshold of 0.7. The interaction network was mapped using Cytoscape (3.8.2).

Gene Set Enrichment Analysis. To interpret the alerted biological functions among the progressive stages of COVID-19 in a protein-expression-dependent manner, we performed gene set enrichment analysis (GSEA). Briefly, proteins were

ranked according to their differences in expression between two categories of clinical disease status (SSEP vs MS, MS vs HC, or SSEP vs HC) and subsequently used as input data for GSEA. First, the protein list was queried against pre-defined gene sets in the GO database to associate gene expression with biological functions. By sequential analysis of the listed proteins, the running-sum statistic was elevated by the GSEA algorithm in a protein-expression-dependent fashion when encountering a protein belonging to a gene set; otherwise, the preceding statistic was reduced at a constant rate. Enrichment score (ES) was defined as the maximum deviation of the running-sum statistic from zero. The *P*-value (without multiplicity adjustment) cutoff was set to 0.1 for determining the significantly enriched pathways. GO terms with the top 10 most significant *P*-values were considered to be the pivotal pathways responsible for the progression of COVID-19, and

Table 2. List of Proteins Dysregulated in All the SARS-CoV-2 Infected Patients

accession	unique peptides	gene	$-\log$ (P-value)	\log (2, NS/HC)	$-\log$ (P-value)	\log (2, MS/HC)	$-\log$ (P-value)	\log (2, SSEP/HC)	$-\log$ (P-value)	\log (2, SSLP/HC)
O75882	50	ATRN	3.355	-1.500	6.052	-2.077	3.142	-1.981	7.019	-2.437
P01042	46	KNG1	3.870	-1.987	2.755	-1.616	3.286	-1.987	4.045	-1.957
P02652	14	APOA2	2.839	-1.238	3.365	-1.697	2.571	-1.911	3.994	-2.280
P02747	7	C1QC	2.494	-1.804	3.109	-1.962	1.986	-1.773	3.130	-2.137
P02760	27	AMBP	2.606	-1.717	1.871	-1.472	2.451	-2.007	2.525	-1.846
P04180	9	LCAT	2.166	-1.346	3.605	-1.863	2.404	-1.615	4.637	-2.115
P05546	29	SERPIND1	2.342	-1.620	2.160	-1.420	2.718	-2.266	2.405	-1.870
P06276	14	BCHE	2.238	-1.643	3.680	-1.532	3.160	-1.974	4.902	-2.230
P06396	41	GSN	2.459	1.476	1.600	1.569	2.526	0.779	1.629	0.668
P06727	67	APOA4	1.787	-1.486	3.230	-2.089	2.438	-1.524	2.399	-1.391
P07225	30	PROS1	2.021	-1.478	2.275	-1.732	2.023	-1.862	2.888	-1.980
P08185	11	SERPINA6	1.912	-0.823	3.083	-1.517	3.450	-2.267	4.501	-2.322
P19823	51	ITIH2	3.248	-1.808	4.076	-1.851	2.760	-2.099	4.434	-2.104
P19827	38	ITIH1	2.582	-1.590	3.601	-1.409	2.670	-1.845	3.347	-2.096
P43652	58	AFM	2.919	-1.767	4.027	-1.817	2.965	-1.933	3.603	-2.014
P54108	7	CRISP3	2.112	-1.280	1.701	-1.212	2.596	-1.797	1.183	-1.315
Q12913	6	PTPRJ	1.768	-0.928	1.958	-1.009	2.546	-2.063	3.622	-2.271
Q5VZ66	2	JAKMIP3	4.319	2.310	5.323	1.350	3.331	1.906	2.290	0.921
Q9NQW8	1	CNGB3	2.333	-1.339	3.315	-1.384	2.365	-1.828	5.941	-2.533

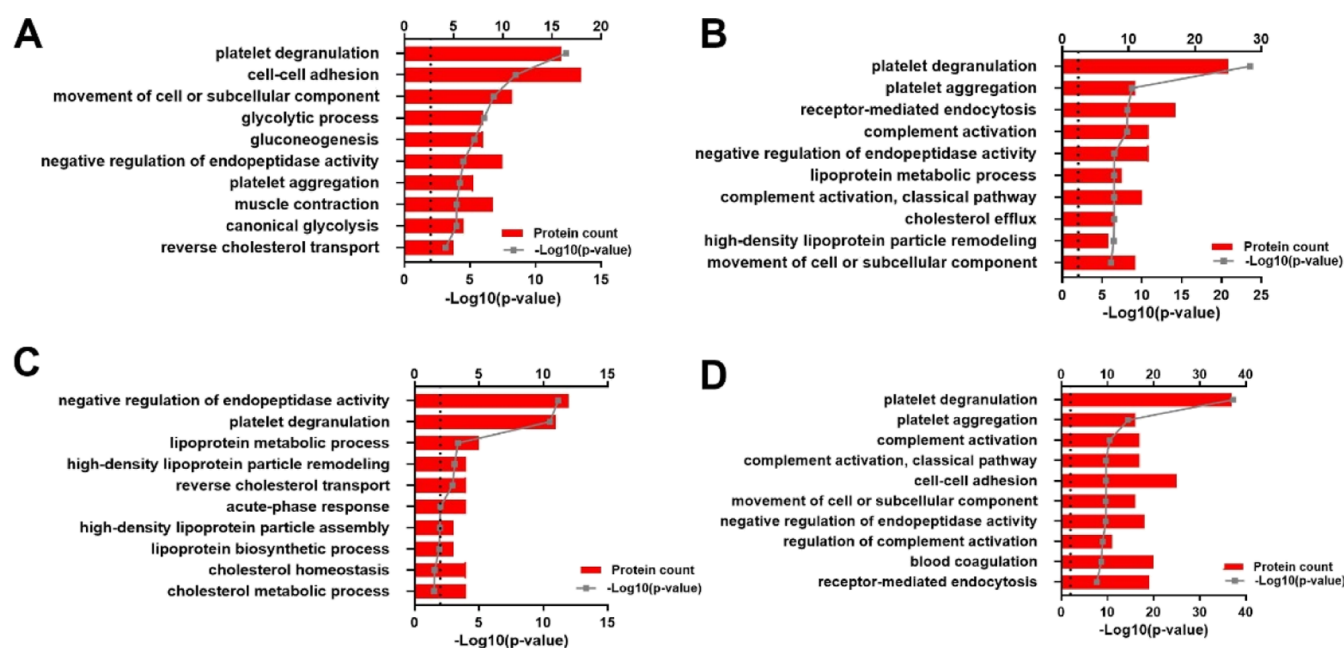


Figure 2. Biological process analysis of the dysregulated plasma proteins of COVID-19 patients. GO analysis of the dysregulated proteins identified in the (A) asymptomatic (NS), (B) MS, (C) SSEP, and (D) SSLP patients. The top 10 items of biological process are listed based on *P*-values together with related protein counts.

the proteins that presented in the leading-edge subsets of the pivotal pathways were defined as core proteins.

ELISA and Receiver Operating Characteristic (ROC) Curve Analysis. ELISA analysis was performed in a BSL-3 laboratory using commercially available kits according to the manufacturer's instructions. Briefly, the plasma samples were diluted to 1:10 for SOD1 (Cloud-Clone, Wuhan China), 1:20 for LDHA (Cloud-Clone, Wuhan China), and 1:250 for PRDX2 (Cloud-Clone, Wuhan China). The samples were added into 96-well plates and incubated with immobilized antibodies. The results were read with a microplate reader (Tecan, Infinite M1000, Switzerland) at an absorbance of 540 nm. Data analysis was performed using GraphPad Prism

(GraphPad Software, San Diego, CA, USA, version 8.2.1). Receiver operating characteristic (ROC) curves were constructed for analysis of the discriminatory power of the candidate markers. Pearson correlation analysis was performed to evaluate the associations between SOD1 and the clinical indicators. Wilcoxon signed-rank tests were used to evaluate the statistical significance of changes in SOD1, LDHA, and PRDX2 expression between HC individuals and patients in the different stages of COVID-19 infection.

Statistical Analysis. For the TMT-labeled proteomic data, paired *t*-tests were used to evaluate the differences between each disease status group and the HC group. Differences among the ELISA results for the groups were evaluated by one-

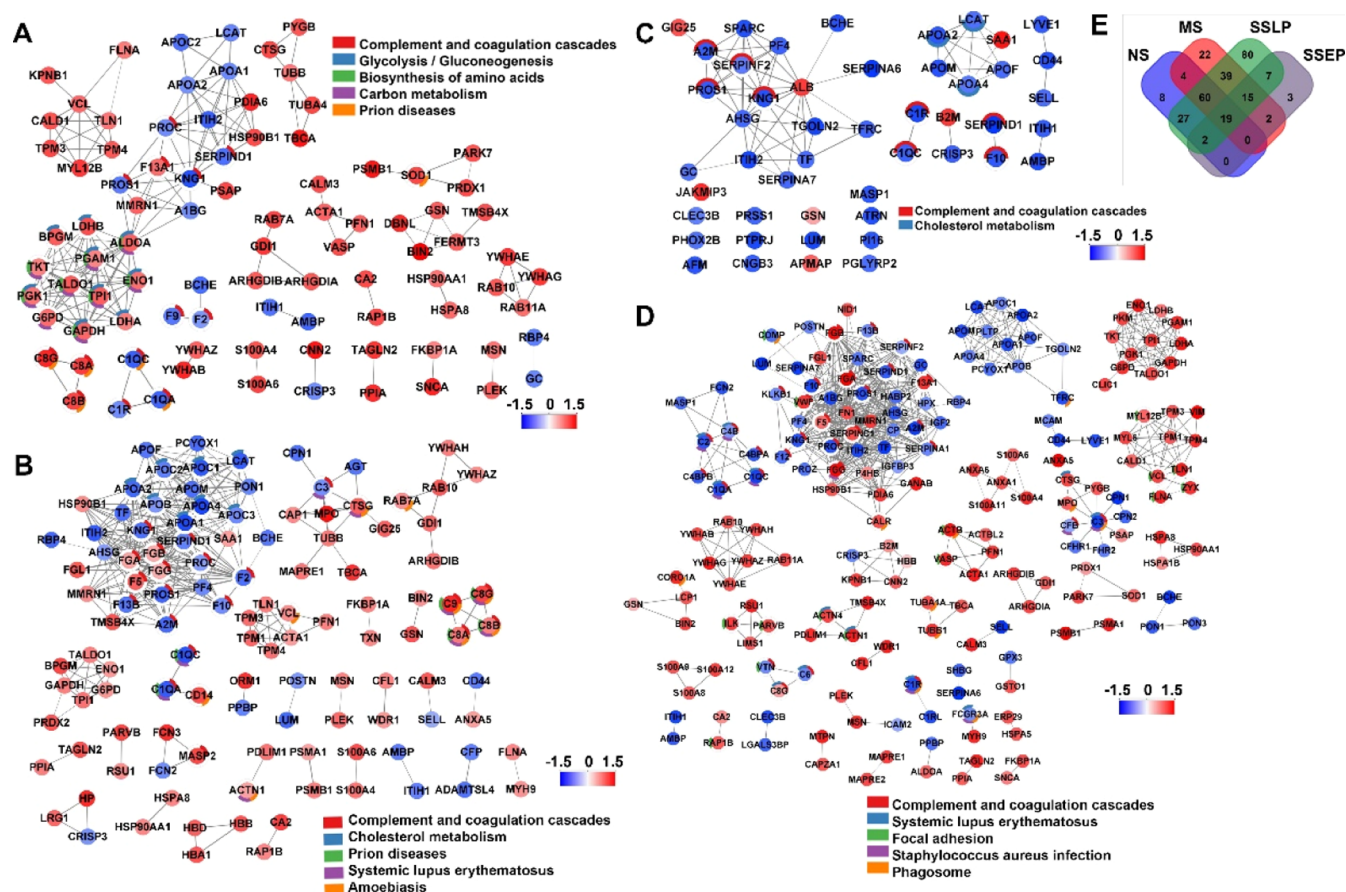


Figure 3. PPIs among the dysregulated proteins in each group analyzed using STRING and the KEGG pathway database. The differentially expressed proteins in the (A) asymptomatic (NS), (B) MS, (C) SSEP, and (D) SSLP groups were analyzed using STRING and the KEGG pathway database compared with the HC group. The upregulated proteins are shown in red and the downregulated proteins are shown in blue. Significantly enriched KEGG pathways are annotated.

way ANOVA. P -values < 0.05 were considered to indicate statistical significance.

RESULTS

Hundreds of Plasma Proteins Were Changed after Infection with SARS-CoV-2. To investigate the changes in the plasma proteome after infection by SARS-CoV-2, the high-abundance plasma proteins were isolated and prepared for proteomic analysis as shown in Figure 1A. In total, 630 plasma proteins from COVID-19 patients and HC individuals were identified and quantified by mass spectrometry with a false discovery rate (FDR) $< 1\%$. 469 plasma proteins were quantified and identified in at least three replicates for data analysis (see Supporting Information Table S1). In order to quantify more peptides, the samples in each batch were split into 15 fractions. Totally, 7944 grouped peptides were quantified and identified from six batches of experiments. Compared with the HC group, hundreds of dysregulated proteins (upregulated and downregulated) were identified in the COVID-19 patient groups. 120 proteins were dysregulated in the NS group compared with those in the HC group, among which 33 proteins were downregulated. The numbers of dysregulated proteins in the MS, SSEP, and SSLP groups were 61, 48, and 249, respectively (see Supporting Information Table S1). Compared with the HC group, two proteins (Gelsolin and Janus kinase and microtubule-interacting protein 3, JAKMIP3) were significantly upregulated and 17 proteins

were downregulated in all the SARS-CoV-2-infected patients. As shown in Figure 1B–F, the plasma proteome was highly dysregulated in all patients after infection by SARS-CoV-2, except in the SSEP group. The significantly dysregulated proteins are shown in Figure 1 and listed in Table 2.

GO Analysis of the Dysregulated Proteins. To understand their functional roles, we performed GO enrichment analysis of all the dysregulated proteins. The top 10 enriched items from the biological process category with a P -value < 0.01 are shown in Figure 2, and those from the cellular component and molecular function categories are shown in Figure S1. GO biological process analysis revealed a high level of similarity among the enriched items in the NS and SSLP groups. The top enriched biological process items in these two groups were platelet degranulation, cell–cell adhesion, movement of cell or subcellular components, and negative regulation of endopeptidase activity. The enriched biological process items in the SSEP group were negative regulation of endopeptidase activity, platelet degranulation, and lipoprotein metabolic process. The cellular component analysis revealed that the dysregulated proteins were enriched in the extracellular exosome, blood microparticles, and the extracellular region in all the investigated groups. The enriched items in the SSLP group were very similar to those in the NS group (Figure S1). Cadherin binding involved in cell–cell adhesion, actin binding, and serine-type endopeptidase inhibitor activity were enriched in the NS, MS, and SSLP groups. Thus, GO

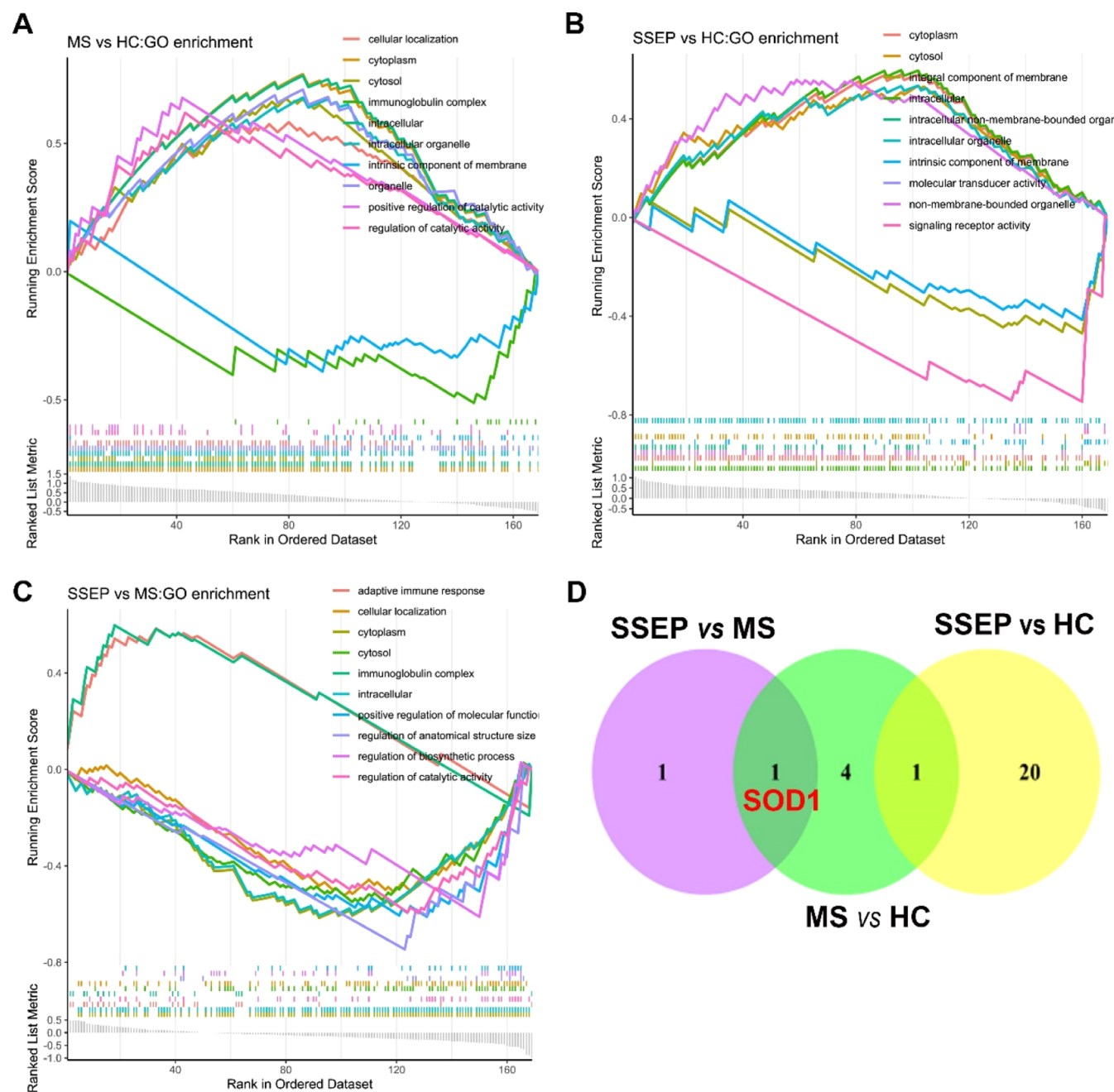


Figure 4. GSEA of the dysregulated proteins in the different clinical stages of COVID-19. Plots of running-sum statistics are shown. (A) GSEA of MS vs HC groups, (B) GSEA of SSEP vs HC groups, and (C) GSEA of SSEP vs MS groups; the bar codes indicate the encountered proteins in the pivotal pathways. (D) Venn diagram showing the intersections of the core proteins identified by GSEA between (among) the three pairs of disease stages. SOD1 is the only core protein that contributed to the core enrichment of all the pivotal pathways in GSEA of both SSEP vs MS and MS vs HC groups.

analysis indicated that the dysregulated proteins in the SSEP group were distinct from those in the other groups.

Dysregulated Proteins Indicated Close PPIs. To investigate the relationship between the PPI connectivity and functional significance, we also performed KEGG pathway analysis of the dysregulated proteins. The dysregulated proteins showed close interactions in the PPIs. The most significantly changed pathway in all groups was complement and coagulation cascades (Figure 3). Glycolysis/gluconeogenesis related proteins were also significantly changed in the NS group (Figure 3A). In the MS group, cholesterol metabolism-related proteins were downregulated, including

APOA1, APOA2, APOC, APOM, and LCAT. Fewer proteins were dysregulated in the SSEP group and cholesterol metabolism related proteins were also enriched as in the MS group (Figure 3C). More proteins were dysregulated in the SSLP group, and complement and coagulation cascades, Staphylococcus aureus infection, and focal adhesion were identified as the dysregulated KEGG pathways (Figure 3D). All the dysregulated KEGG pathway analyses are shown in Figure S2 and Table S2.

SOD1 as a Pivotal Indicator for the Severity of COVID-19. To compare the dysregulated proteins among the different clinical disease status groups, we performed the GSEA

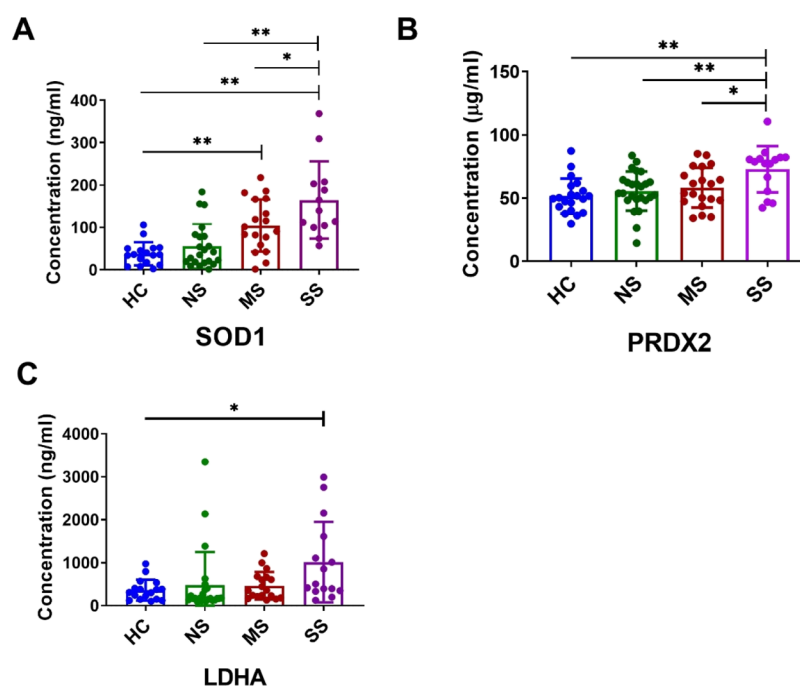


Figure 5. ELISA validation of dysregulated proteins identified by mass spectrometry. Plasma proteins from HCs ($n = 19$), asymptomatic (NS, $n = 24$), and MS ($n = 20$), and severe syndrome (SS, $n = 15$) patients were verified by ELISA analysis. (A) SOD1, (B) PRDX2, and (C) LDHA were analyzed using an unpaired student's *t*-tests for the significance comparison; * $P < 0.05$, ** $P < 0.01$.

on the MS versus HC groups, the SSEP versus HC groups, and the SSEP versus MS group. The top 10 enriched pathways (with the highest P -value) in the three GSEAs were designated as the pivotal pathways; the corresponding running enrichment scores are shown in Figure 4A–C. These results indicated that biological alterations across different COVID-19 stages were clustered in the cytoplasm-associated pathways; details of the core enrichment sites are provided in Supporting Information Tables S3–S5. We defined the proteins present in the core enrichment sites of all the pivotal pathways of a GSEA as the core proteins, and then focused on the intersections of core proteins between any two GSEAs. As shown in Figure 4, SOD1 was the only protein that contributed to the core enrichment of the pivotal pathways in GSEA of both the MS versus HC groups and the SSEP versus MS groups, suggesting that SOD1 was a pivotal indicator for the severity of COVID-19.

Verification of Protein Expression Levels by ELISA. To validate the accuracy of the MS data, we analyzed the levels of three proteins (SOD1, LDHA, and PRDX2) in individual plasma samples by ELISA. Detailed information for the samples is listed in Tables 1 and S6. We found that SOD1 levels were significantly changed in the MS and SS groups, but not in the NS group. PRDX2 and LDHA levels were increased in the SS group, but not in the other groups (Figure 5). Thus, the results of the ELISA analyses were consistent with the MS data.

SOD1 was Used to Distinguish Patients with Infections from HCs. The ROC analysis demonstrated the value of SOD1 for distinguishing patients with SARS-CoV-2 infection from HCs, with a specificity and sensitivity of 89.5% and 88.9%, respectively, and an area under curve (AUC) of 90.9% (Figure 6A). Furthermore, SOD1 was shown to distinguish the MS group from the HC group with a specificity and sensitivity of 89.5 and 81.0%, respectively. SOD1 was also shown to distinguish the SS group from the HC group with a

specificity and sensitivity of 100% (Figure 6B,C). In contrast, the ROC curve analysis showed that the specificity and sensitivity of PRDX2 and LDHA for distinguishing patients with SARS-CoV-2 infection from HCs were less than those of SOD1 (Figure S3). Pearson correlation analysis of plasma SOD1 levels and the clinical stages of COVID-19 indicated that the plasma SOD1 was negatively correlated with potassium ($R = -0.58$, $P = 0.012$), but positively correlated with γ -glutamyl transpeptidase (GGT) ($R = 0.67$, $P = 0.024$) and PaCO₂ ($R = 0.57$, $P = 0.013$) in SARS-CoV-2-infected patients (Figure S5–F). These results indicated that plasma SOD1 levels can be used to distinguish patients with COVID-19 from HCs.

DISCUSSION

In this study, we used the TMT-labeling approach to analyze the correlation between the proteomic changes and clinical symptoms of patients with SARS-CoV-2 infection, including those in asymptomatic, mild symptoms, and severe symptoms in the early and later phases. Compared with HCs, we detected changes in hundreds of plasma protein levels in patients with SARS-CoV-2 infection, even in the NS group. Age was one of the important risk factors for the severity of COVID-19 disease;²⁰ while average age in each group we used was different, this could be a potential limitation for this study. Further analysis revealed a high level of similarity in the GO annotations for the changed proteins in the NS, MS, and SSLP groups. The roles of these proteomic changes in SARS-CoV-2-infected individuals, including asymptomatic individuals, require further clarification.

It was reported that oxidative stress-induced cellular damage serves an important role in the respiratory viral infection.²¹ Oxidative stress is considered as one of the key mechanisms responsible for disease severity of COVID-19.^{22,23} Only little information was available about the relationship between

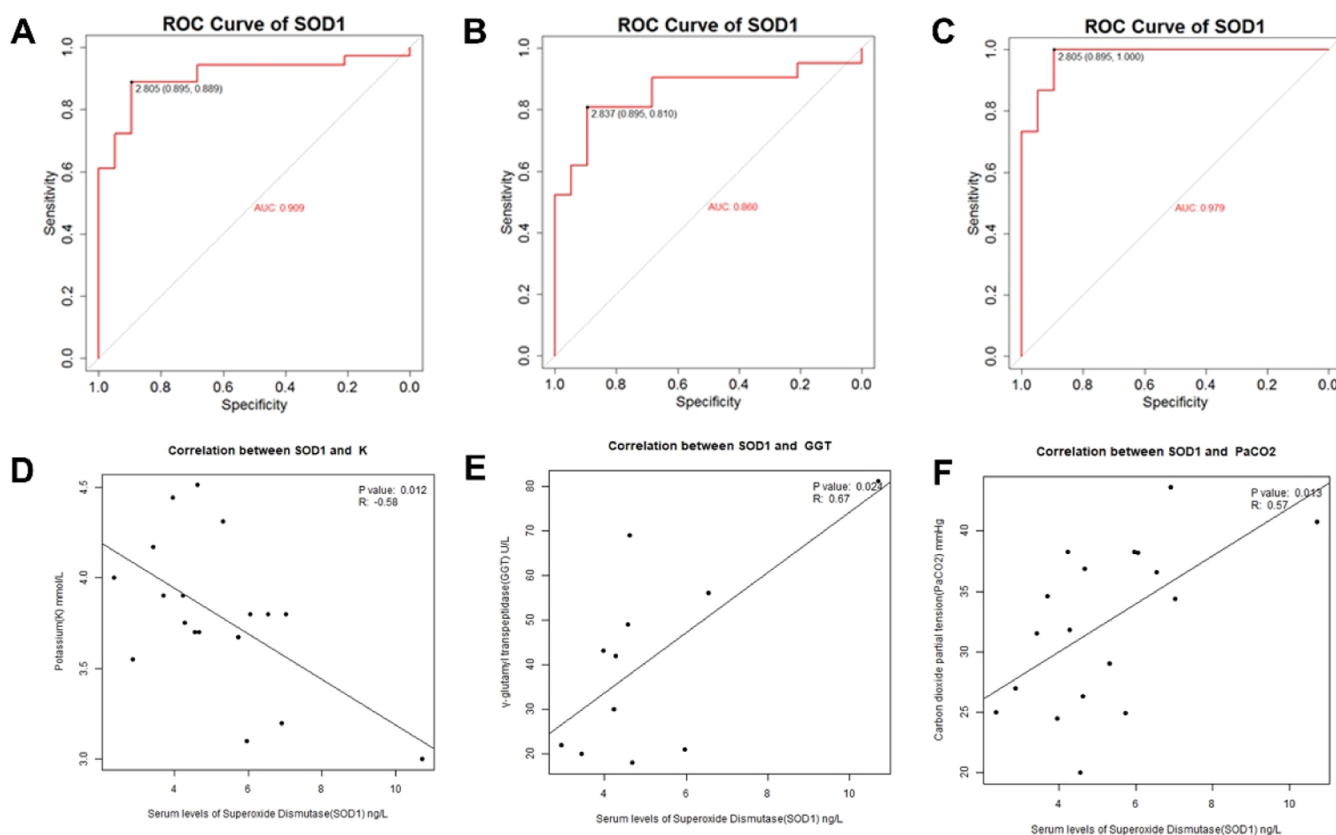


Figure 6. Pivotal roles of SOD1 in the progression of COVID-19. ROC curves revealed the distinguishing ability of SOD1 for COVID-19 infection. (A) Distinguishing patients with SARS-CoV-2 infections from HCs: specificity = 89.5%, sensitivity = 88.9%, AUC = 90.9%. (B) Distinguishing patients with MS from HCs: specificity = 89.5%, sensitivity = 81.0%, AUC = 86.0%. (C) Distinguishing severe syndrome (SS) from HCs: specificity = 89.5%, sensitivity = 100%, AUC = 97.9%. Plasma SOD1 level was associated with potassium, GGT and PaCO₂. (D) Plasma SOD1 levels were negatively correlated with potassium ($R = -0.58$, $P = 0.012$) in SARS-CoV-2-infected individuals. (E) Plasma SOD1 level was positively correlated with GGT ($R = 0.67$, $P = 0.024$) in SARS-CoV-2-infected individuals. (F) Plasma SOD1 levels were positively correlated with PaCO₂ ($R = 0.57$, $P = 0.013$) in SARS-CoV-2-infected individuals.

oxidative stress and COVID-19 disease.^{24,25} SARS-CoV-2 enters the host cell mainly *via* the cell surface enzyme angiotensin-converting enzyme 2 (ACE2), which plays a pivotal role in the conversion of angiotensin II (ANG II) to ANG-(1–7). The interaction of Ang-(1–7) with its receptor Mas plays an important role in the balance between reactive oxygen species (ROS) production and antioxidant capacity.²⁶ Endocytosis of SARS-CoV-2 particles results in the downregulation of active ACE2 and increased ANG II.²⁷ Thus, SARS-CoV-2 infection induces severe inflammation and ROS production, which trigger damage to the infected organs. Superoxide dismutases (SODs) and peroxiredoxin family members (PRXs) function as antioxidant enzymes.²⁸ A recent study using a single-cell RNA sequencing method indicated that SOD3 was downregulated in lung cells from COVID-19 patients.²⁴ However, the roles of antioxidant enzymes in the human body after infection with SARS-CoV-2 remain to be fully elucidated. In our study, we found that SOD1 and PRDX2 were enriched in the plasma of COVID-19 patients, especially in severe cases. Our GSEA of both the MS versus HC groups and the SSEP versus MS groups also revealed dysregulation of SOD1. Given that SOD1 was the only protein found to contribute to the pivotal pathways in GSEA of both the SSEP versus MS groups and the MS versus HC groups, we hypothesized that SOD1 is the crucial link between the different progressive stages of COVID-19. Experimental validation (ELISA) of SOD1 levels also showed that SOD1

offers a relatively high AUC (>0.9) in distinguishing infected individuals from HCs, which further corroborated the GSEA results. Thus, these findings indicate that the oxidative stress balance is disrupted after infection with SARS-CoV-2. In addition, it was reported that hypokalemia is associated with the severe progression of COVID-19.²⁹ In our study, we found that SOD1 was negatively associated with the plasma potassium levels in patients with COVID-19 pneumonia. It can be speculated that the combination of plasma levels of potassium and SOD1 may be a more sensitive indicator of the progression of COVID-19. Thus, SOD1 could be an important indicator for the prediction of disease severity in COVID-19. However, only a small number of patients were enrolled in this study and this association remains to be confirmed in a larger cohort study.

COVID-19 research is complicated by the diversity of symptoms exhibited by individuals infected by SARS-CoV-2. Type 2 diabetes (T2D) and other metabolic conditions closely related to elevated glucose levels are among the risk factors for severe symptoms.^{30,31} It has been confirmed that glycolysis is necessary for the replication of SARS-CoV-2 and glycolysis-related genes are upregulated during infection.³² Clinical evidence has also proven that glucose control is a useful strategy to improve outcomes for COVID-19 patients.³¹ In this study, we also found that glycolysis-related protein levels were increased in COVID-19 patients compared with those in HCs. Alpha-enolase (ENO1) is a multifunctional protein that is not

only a glycolytic enzyme, but also functions as a heat-shock protein and a hypoxic stress protein. The roles of ENO1 in the replication and infection processes of different viruses are unclear. However, ENO1 has been identified as a negative regulatory factor for HIV-1 reverse transcription.³³ Our proteomic analysis revealed that plasma ENO1 levels were increased in COVID-19 patients, thus indicating that ENO1 also plays a role in SARS-CoV-2 infection.

As a component of both innate and adaptive immunity, the complement system plays a critical role in the detection and removal of invading pathogens.^{34,35} Both *in vivo* and *in vitro* studies have suggested that complement activation is involved in the pathogenesis and severity of COVID-19.³⁴ Compared with wild-type mice, lung injury and weight loss were significantly reduced in C3^{-/-} mice after infection with SARS-CoV-2.³⁶ Multiple therapeutic agents that inhibit complement activation are being investigated and show promise for the treatment of COVID-19.³⁷ However, regulation of the complement system and the most appropriate point for effective complement intervention remain to be established. Our proteomic analysis also revealed dysregulation of the complement system, with decreased levels of C1q and C3 and increased levels of C9 in the plasma of COVID-19 patients compared with those in HCs. Thus, the use of complement activation inhibitors should be applied with caution.

CONCLUSIONS

In this study, we conducted a comprehensive proteomic study on the plasma of COVID-19 patients with a range of clinical symptoms. Our results indicated that the landscape of proteins changes after infection with SARS-CoV-2. The dysregulated pathways involved should be carefully considered when COVID-19 patients are diagnosed and treated. In particular, oxidative stress and SOD1 may play an important role in the stage of disease after infection by SARS-CoV-2.

ASSOCIATED CONTENT

Supporting Information

The Supporting Information is available free of charge at <https://pubs.acs.org/doi/10.1021/acsomega.1c01375>.

GO analysis of the dysregulated plasma proteins in COVID-19 patients; KEGG pathway analysis of the dysregulated proteins; and ROC curves revealing the distinguishing ability of LDHA or PRDX2 for COVID-19 infection (PDF)

List of all the significantly dysregulated proteins; KEGG pathway analysis of the dysregulated proteins from COVID-19 infection patients and controls; GO analysis of the dysregulated proteins from MS and HC groups; GO analysis of the dysregulated proteins from SSEP and HC groups; GO analysis of the dysregulated proteins from SSEP and MS groups; and detailed information for patients and HCs (XLSX)

AUTHOR INFORMATION

Corresponding Authors

Jianjun Liu – Shenzhen Center for Disease Control and Prevention, Shenzhen 518055, China; orcid.org/0000-0002-9662-8294; Email: toxic_01@szcdc.net

Shisong Fang – Shenzhen Center for Disease Control and Prevention, Shenzhen 518055, China; Email: szcdcssf@aliyun.com

Zigang Li – State Key Laboratory of Chemical Oncogenomics, School of Chemical Biology and Biotechnology, Peking University Shenzhen Graduate School, Shenzhen 518055, China; Pingshan Translational Medicine Center, Shenzhen Bay Laboratory, Shenzhen 518101, China; orcid.org/0000-0002-3630-8520; Email: lizg@pkusz.edu.cn

Authors

Benhong Xu – Shenzhen Center for Disease Control and Prevention, Shenzhen 518055, China

Yuxuan Lei – Shenzhen Center for Disease Control and Prevention, Shenzhen 518055, China; School of Public Health (Shenzhen), Sun Yat-sen University, Guangzhou 510275, China

Xiaohu Ren – Shenzhen Center for Disease Control and Prevention, Shenzhen 518055, China

Feng Yin – State Key Laboratory of Chemical Oncogenomics, School of Chemical Biology and Biotechnology, Peking University Shenzhen Graduate School, Shenzhen 518055, China; Pingshan Translational Medicine Center, Shenzhen Bay Laboratory, Shenzhen 518101, China

Weihua Wu – Shenzhen Center for Disease Control and Prevention, Shenzhen 518055, China

Ying Sun – Shenzhen Center for Disease Control and Prevention, Shenzhen 518055, China

Xiaohui Wang – Shenzhen Center for Disease Control and Prevention, Shenzhen 518055, China

Qian Sun – Shenzhen Center for Disease Control and Prevention, Shenzhen 518055, China

Xifei Yang – Shenzhen Center for Disease Control and Prevention, Shenzhen 518055, China; orcid.org/0000-0002-9000-7016

Xin Wang – Shenzhen Center for Disease Control and Prevention, Shenzhen 518055, China

Renli Zhang – Shenzhen Center for Disease Control and Prevention, Shenzhen 518055, China

Complete contact information is available at:

<https://pubs.acs.org/doi/10.1021/acsomega.1c01375>

Author Contributions

B.H.X., Y.X.L., and X.H.R. contributed equally. J.J.L., S.S.F., and X.F.Y. designed the study. B.H.X., Y.X.L., and X.H.R. performed the experiments and data analysis. B.H.X. prepared the manuscript. F. Y., W.H.W., Y.S., Q.S., X.W., R.L.Z., and Z.G.L. prepared the samples and participated in the data analysis and manuscript revision.

Notes

The authors declare no competing financial interest.

ACKNOWLEDGMENTS

This project was supported by Open Program of Shenzhen Bay Laboratory (SZBL202002271005), Shenzhen Key Medical Discipline Construction Fund (SZXK069), the Guangdong Natural Science Foundation (2018A030313242), and Sanming Project of Medicine in Shenzhen (SZSM201611090).

REFERENCES

- <https://www.who.int/director-general/speeches/detail/who-director-general-s-opening-remarks-at-the-media-briefing-on-covid-19---11-march-2020> (accessed on March 16, 2021).

- (2) <https://coronavirus.jhu.edu/map.html> (accessed on March 16, 2021).
- (3) Kirenga, B.; Muttamba, W.; Kayongo, A.; Nsereko, C.; Siddharthan, T.; Lusiba, J.; Mugenyi, L.; Byanyima, R. K.; Worodria, W.; Nakwagala, F.; Nantanda, R.; Kimuli, I.; Katagira, W.; Bagaya, B. S.; Nasinghe, E.; Aanyu-Tukamuhebwa, H.; Amuge, B.; Sekibira, R.; Buregyeya, E.; Kiwanuka, N.; Muwanga, M.; Kalungi, S.; Joloba, M. L.; Kateete, D. P.; Byarugaba, B.; Kanya, M. R.; Mwebesa, H.; Bazeyo, W. Characteristics and outcomes of admitted patients infected with SARS-CoV-2 in Uganda. *BMJ Open Respir. Res.* **2020**, *7*, No. e000646.
- (4) Guan, W.-J.; Ni, Z.-Y.; Hu, Y.; Liang, W.-H.; Ou, C.-Q.; He, J.-X.; Liu, L.; Shan, H.; Lei, C.-L.; Hui, D. S. C.; Du, B.; Li, L.-J.; Zeng, G.; Yuen, K.-Y.; Chen, R.-C.; Tang, C.-L.; Wang, T.; Chen, P.-Y.; Xiang, J.; Li, S.-Y.; Wang, J.-L.; Liang, Z.-J.; Peng, Y.-X.; Wei, L.; Liu, Y.; Hu, Y.-H.; Peng, P.; Wang, J.-M.; Liu, J.-Y.; Chen, Z.; Li, G.; Zheng, Z.-J.; Qiu, S.-Q.; Luo, J.; Ye, C.-J.; Zhu, S.-Y.; Zhong, N.-S.; China Medical Treatment Expert Group for, C.. Clinical Characteristics of Coronavirus Disease 2019 in China. *N. Engl. J. Med.* **2020**, *382*, 1708–1720.
- (5) Mayr, M.; Zhang, J.; Greene, A. S.; Gutterman, D.; Perloff, J.; Ping, P. Proteomics-based development of biomarkers in cardiovascular disease: mechanistic, clinical, and therapeutic insights. *Mol. Cell. Proteomics* **2006**, *5*, 1853–1864.
- (6) Bader, J. M.; Geyer, P. E.; Müller, J. B.; Strauss, M. T.; Koch, M.; Leypoldt, F.; Koertvelyessy, P.; Bittner, D.; Schipke, C. G.; Incesoy, E. I.; Peters, O.; Deigendesch, N.; Simons, M.; Jensen, M. K.; Zetterberg, H.; Mann, M. Proteome profiling in cerebrospinal fluid reveals novel biomarkers of Alzheimer's disease. *Mol. Syst. Biol.* **2020**, *16*, No. e9356.
- (7) Keshishian, H.; Burgess, M. W.; Specht, H.; Wallace, L.; Clauser, K. R.; Gillette, M. A.; Carr, S. A. Quantitative, multiplexed workflow for deep analysis of human blood plasma and biomarker discovery by mass spectrometry. *Nat. Protoc.* **2017**, *12*, 1683–1701.
- (8) Ren, Y.; He, Q.-Y.; Fan, J.; Jones, B.; Zhou, Y.; Xie, Y.; Cheung, C.-Y.; Wu, A.; Chiu, J.-F.; Peiris, J. S. M.; Tam, P. K. H. The use of proteomics in the discovery of serum biomarkers from patients with severe acute respiratory syndrome. *Proteomics* **2004**, *4*, 3477–3484.
- (9) Rana, R.; Rath, V.; Ganguly, N. K. A comprehensive overview of proteomics approach for COVID 19: new perspectives in target therapy strategies. *J. Proteins Proteomics* **2020**, *11*, 223–232.
- (10) Kim, G. U.; Kim, M. J.; Ra, S. H.; Lee, J.; Bae, S.; Jung, J.; Kim, S. H. Clinical characteristics of asymptomatic and symptomatic patients with mild COVID-19. *Clin. Microbiol. Infect.* **2020**, *26*, 948.e1–948.e3.
- (11) Suleyman, G.; Fadel, R. A.; Malette, K. M.; Hammond, C.; Abdulla, H.; Entz, A.; Demertzis, Z.; Hanna, Z.; Failla, A.; Dagher, C.; Chaudhry, Z.; Vahia, A.; Abreu Lanfranco, O.; Ramesh, M.; Zervos, M. J.; Alangaden, G.; Miller, J.; Brar, I. Clinical Characteristics and Morbidity Associated With Coronavirus Disease 2019 in a Series of Patients in Metropolitan Detroit. *JAMA Netw. Open* **2020**, *3*, No. e2012270.
- (12) Gebhard, C.; Regitz-Zagrosek, V.; Neuhauser, H. K.; Morgan, R.; Klein, S. L. Impact of sex and gender on COVID-19 outcomes in Europe. *Biol. Sex Differ.* **2020**, *11*, 29.
- (13) Shu, T.; Ning, W.; Wu, D.; Xu, J.; Han, Q.; Huang, M.; Zou, X.; Yang, Q.; Yuan, Y.; Bie, Y.; Pan, S.; Mu, J.; Han, Y.; Yang, X.; Zhou, H.; Li, R.; Ren, Y.; Chen, X.; Yao, S.; Qiu, Y.; Zhang, D.-Y.; Xue, Y.; Shang, Y.; Zhou, X. Plasma Proteomics Identify Biomarkers and Pathogenesis of COVID-19. *Immunity* **2020**, *53*, 1108–1122.e5.
- (14) Shen, B.; Yi, X.; Sun, Y.; Bi, X.; Du, J.; Zhang, C.; Quan, S.; Zhang, F.; Sun, R.; Qian, L.; Ge, W.; Liu, W.; Liang, S.; Chen, H.; Zhang, Y.; Li, J.; Xu, J.; He, Z.; Chen, B.; Wang, J.; Yan, H.; Zheng, Y.; Wang, D.; Zhu, J.; Kong, Z.; Kang, Z.; Liang, X.; Ding, X.; Ruan, G.; Xiang, N.; Cai, X.; Gao, H.; Li, L.; Li, S.; Xiao, Q.; Lu, T.; Zhu, Y.; Liu, H.; Chen, H.; Guo, T. Proteomic and Metabolomic Characterization of COVID-19 Patient Sera. *Cell* **2020**, *182*, 59–72.e15.
- (15) Lin, B.; Liu, J.; Liu, Y.; Qin, X. Progress in understanding COVID-19: insights from the omics approach. *Crit. Rev. Clin. Lab. Sci.* **2021**, *58*, 242–252.
- (16) Grenga, L.; Armengaud, J. Proteomics in the COVID-19 Battlefield: First Semester Check-Up. *Proteomics* **2021**, *21*, No. e2000198.
- (17) Liu, Y.; Zhang, C.; Huang, F.; Yang, Y.; Wang, F.; Yuan, J.; Zhang, Z.; Qin, Y.; Li, X.; Zhao, D.; Li, S.; Tan, S.; Wang, Z.; Li, J.; Shen, C.; Li, J.; Peng, L.; Wu, W.; Cao, M.; Xing, L.; Xu, Z.; Chen, L.; Zhou, C.; Liu, W. J.; Liu, L.; Jiang, C. Elevated plasma levels of selective cytokines in COVID-19 patients reflect viral load and lung injury. *Natl. Sci. Rev.* **2020**, *7*, 1003–1011.
- (18) Xu, B.; Zheng, C.; Chen, X.; Zhang, Z.; Liu, J.; Spencer, P.; Yang, X. Dysregulation of Myosin Complex and Striated Muscle Contraction Pathway in the Brains of ALS-SOD1 Model Mice. *ACS Chem. Neurosci.* **2019**, *10*, 2408–2417.
- (19) Perez-Riverol, Y.; Csordas, A.; Bai, J.; Bernal-Llinares, M.; Hewapathirana, S.; Kundu, D. J.; Inuganti, A.; Griss, J.; Mayer, G.; Eisenacher, M.; Pérez, E.; Uszkoreit, J.; Pfeuffer, J.; Sachsenberg, T.; Yilmaz, Ş.; Tiwary, S.; Cox, J.; Audain, E.; Walzer, M.; Jarnuczak, A. F.; Ternent, T.; Brazma, A.; Vizcaino, J. A. The PRIDE database and related tools and resources in 2019: improving support for quantification data. *Nucleic Acids Res.* **2019**, *47*, D442–D450.
- (20) Angioni, R.; Sánchez-Rodríguez, R.; Munari, F.; Bertoldi, N.; Arcidiacono, D.; Cavinato, S.; Marturano, D.; Zaramella, A.; Realdon, S.; Cattelan, A.; Viola, A.; Molon, B. Age-severity matched cytokine profiling reveals specific signatures in Covid-19 patients. *Cell Death Dis.* **2020**, *11*, 957.
- (21) Komaravelli, N.; Casola, A. Respiratory Viral Infections and Subversion of Cellular Antioxidant Defenses. *J. Pharmacogenomics Pharmacoproteomics* **2014**, *5*, 1000141.
- (22) Laforge, M.; Elbim, C.; Frère, C.; Hémadi, M.; Massaad, C.; Nuss, P.; Benoliel, J.-J.; Becker, C. Tissue damage from neutrophil-induced oxidative stress in COVID-19. *Nat. Rev. Immunol.* **2020**, *20*, 515–516.
- (23) Delgado-Roche, L.; Mesta, F. Oxidative Stress as Key Player in Severe Acute Respiratory Syndrome Coronavirus (SARS-CoV) Infection. *Arch. Med. Res.* **2020**, *51*, 384–387.
- (24) Abouhashem, A. S.; Singh, K.; Azzazy, H. M. E.; Sen, C. K. Is Low Alveolar Type II Cell SOD3 in the Lungs of Elderly Linked to the Observed Severity of COVID-19? *Antioxid. Redox Signaling* **2020**, *33*, 59–65.
- (25) Kalem, A. K.; Kayaaslan, B.; Neselioglu, S.; Eser, F.; Hasanoglu, İ.; Aypak, A.; Akinci, E.; Akca, H. N.; Erel, O.; Guner, R. A useful and sensitive marker in the prediction of COVID-19 and disease severity: Thioli. *Free Radical Biol. Med.* **2021**, *166*, 11–17.
- (26) Rabelo, L. A.; Alenina, N.; Bader, M. ACE2–angiotensin-(1–7)–Mas axis and oxidative stress in cardiovascular disease. *Hypertens. Res.* **2011**, *34*, 154–160.
- (27) Dong, S.; Liu, P.; Luo, Y.; Cui, Y.; Song, L.; Chen, Y. Pathophysiology of SARS-CoV-2 infection in patients with intracerebral hemorrhage. *Aging* **2020**, *12*, 13791–13802.
- (28) Henkle-Dührsen, K.; Kampkötter, A. Antioxidant enzyme families in parasitic nematodes. *Mol. Biochem. Parasitol.* **2001**, *114*, 129–142.
- (29) Moreno-Pérez, O.; Leon-Ramirez, J.-M.; Fuertes-Kenneally, L.; Perdiguer, M.; Andres, M.; Garcia-Navarro, M.; Ruiz-Torregrosa, P.; Boix, V.; Gil, J.; Merino, E. Hypokalemia as a sensitive biomarker of disease severity and the requirement for invasive mechanical ventilation requirement in COVID-19 pneumonia: A case series of 306 Mediterranean patients. *Int. J. Infect. Dis.* **2020**, *100*, 449–454.
- (30) Ayres, J. S. A metabolic handbook for the COVID-19 pandemic. *Nat. Metab.* **2020**, *2*, 572–585.
- (31) Zhu, L.; She, Z.-G.; Cheng, X.; Qin, J.-J.; Zhang, X.-J.; Cai, J.; Lei, F.; Wang, H.; Xie, J.; Wang, W.; Li, H.; Zhang, P.; Song, X.; Chen, X.; Xiang, M.; Zhang, C.; Bai, L.; Xiang, D.; Chen, M.-M.; Liu, Y.; Yan, Y.; Liu, M.; Mao, W.; Zou, J.; Liu, L.; Chen, G.; Luo, P.; Xiao, B.; Zhang, C.; Zhang, Z.; Lu, Z.; Wang, J.; Lu, H.; Xia, X.; Wang, D.; Liao, X.; Peng, G.; Ye, P.; Yang, J.; Yuan, Y.; Huang, X.; Guo, J.;

Zhang, B.-H.; Li, H. Association of Blood Glucose Control and Outcomes in Patients with COVID-19 and Pre-existing Type 2 Diabetes. *Cell Metab.* **2020**, *31*, 1068–1077.e3.

(32) Codo, A. C.; Davanzo, G. G.; Monteiro, L. d. B.; de Souza, G. F.; Muraro, S. P.; Virgilio-da-Silva, J. V.; Prodonoff, J. S.; Carregari, V. C.; de Biagi Junior, C. A. O.; Crunfli, F.; Jimenez Restrepo, J. L.; Vendramini, P. H.; Reis-de-Oliveira, G.; Bispo Dos Santos, K.; Toledo-Teixeira, D. A.; Parise, P. L.; Martini, M. C.; Marques, R. E.; Carmo, H. R.; Borin, A.; Coimbra, L. D.; Boldrini, V. O.; Brunetti, N. S.; Vieira, A. S.; Mansour, E.; Ulaf, R. G.; Bernardes, A. F.; Nunes, T. A.; Ribeiro, L. C.; Palma, A. C.; Agrela, M. V.; Moretti, M. L.; Sposito, A. C.; Pereira, F. B.; Velloso, L. A.; Vinolo, M. A. R.; Damasio, A.; Proença-Módena, J. L.; Carvalho, R. F.; Mori, M. A.; Martins-de-Souza, D.; Nakaya, H. I.; Farias, A. S.; Moraes-Vieira, P. M. Elevated Glucose Levels Favor SARS-CoV-2 Infection and Monocyte Response through a HIF-1 α /Glycolysis-Dependent Axis. *Cell Metab.* **2020**, *32*, 437–446.e5.

(33) Kishimoto, N.; Iga, N.; Yamamoto, K.; Takamune, N.; Misumi, S. Virion-incorporated alpha-enolase suppresses the early stage of HIV-1 reverse transcription. *Biochem. Biophys. Res. Commun.* **2017**, *484*, 278–284.

(34) Java, A.; Apicelli, A. J.; Liszewski, M. K.; Coler-Reilly, A.; Atkinson, J. P.; Kim, A. H.; Kulkarni, H. S., The complement system in COVID-19: friend and foe? *JCI insight* **2020**, *5* (), e140711. DOI: [10.1172/jci.insight.140711](https://doi.org/10.1172/jci.insight.140711)

(35) West, E. E.; Kolev, M.; Kemper, C. Complement and the Regulation of T Cell Responses. *Annu. Rev. Immunol.* **2018**, *36*, 309–338.

(36) Gralinski, L. E.; Sheahan, T. P.; Morrison, T. E.; Menachery, V. D.; Jensen, K.; Leist, S. R.; Whitmore, A.; Heise, M. T.; Baric, R. S. Complement Activation Contributes to Severe Acute Respiratory Syndrome Coronavirus Pathogenesis. *mBio* **2018**, *9*, No. e01753.

(37) Kurtovic, L.; Beeson, J. G. Complement Factors in COVID-19 Therapeutics and Vaccines. *Trends Immunol.* **2021**, *42*, 94–103.